IJL, Issue 2, Vol. 24, 2025
https://doi.org/10.31900/ijl.v24i2.532

Research Article

IRAQI JOURNAL OF LASER

Quantitative Assessment of Laser Pulse Energy Effects on Zn–Cu Plasma Characteristics via Boltzmann and Stark Diagnostics

Sana A. Salah[1], *, Kadhim A. Aadim[2]

[1]*Department of Physics, College of Science, University of Baghdad, Baghdad, Iraq*
[2]*Institute of Laser for Postgraduate Studies, University of Baghdad, Baghdad, Iraq*
**Email address of the Corresponding author*: Sanaa.Abd2304@sc.uobaghdad.edu.iq

Article history: Received 26 Apr. 2025; Revised 27 Jun. 2025; Accepted 3 Jul. 2025; Published online 15 Dec. 2025

Abstract: In this study, laser-induced breakdown spectroscopy (LIBS) was used to analyze the plasma generated from a Zn:Cu alloy (x = 0.9) using a Nd:YAG laser at 1064 nm. Plasma was generated at different laser pulse energies ranging from 400 to 800 mJ. The electron temperature (Te) was determined using the Boltzmann plot method, while the electron number density (ne) was calculated using Stark broadening. Other plasma parameters were also evaluated, including plasma frequency (fp), Debye length (λD), and Debye number (Nd). The results showed that Te increased from 0.846 eV at 400 mJ to 0.906 eV at 800 mJ, and ne increased from 1.000×10^{18} cm^{-3} to 1.121×10^{18} cm^{-3}. Plasma frequency increased from 898.000×10^{10} Hz to $950{,}868 \times 10^{10}$ Hz, while the Debye length slightly decreased from 0.683×10^{-5} cm to 0.668×10^{-5} cm. The Debye number showed modest variation around 1300, reflecting relatively stable collective behavior across the energy range. These findings indicate that higher laser energy leads to hotter and denser plasma, enhancing the emission intensity and plasma characteristics. The study contributes quantitative insights into Zn–Cu plasma behavior under varying laser energies, providing potential applications in material diagnostics using LIBS.

Keywords: LIBS, Zn–Cu alloy, laser-induced plasma, plasma parameters, Boltzmann plot, Stark broadening.

1. Introduction

Laser-Induced Breakdown Spectroscopy (LIBS) is a modern analytical technique widely employed for examining elemental composition and plasma properties across various materials. Its non-destructive nature ensures that the chemical structure of the sample remains unchanged, making LIBS highly applicable in diverse scientific and industrial domains. The method operates by directing a high-energy laser pulse onto the target surface, leading to the ejection of a minute quantity of material and the subsequent generation of a transient, high-temperature plasma plume [1]. This plasma typically comprises free electrons and ions. The electrons, being highly mobile, collide with atoms and ions in the plasma, causing excitation to higher energy levels. These excited species then emit characteristic radiation as they relax back to lower energy states. The emitted light is captured and analyzed by a spectrometer to identify elemental constituents and their relative concentrations [2].

The optical emission from this laser-induced plasma offers crucial diagnostic information, especially regarding electron temperature (T_e) and electron density (n_e), which are vital indicators of plasma

behavior. These parameters are influenced by several factors, including laser wavelength, pulse energy, duration, repetition rate, and the physical and chemical properties of the target material [3, 4]. Understanding how these factors interact is essential for optimizing experimental setups and achieving reliable spectral data.

Copper-zinc (Zn:Cu) alloys are of particular interest due to their multifunctional characteristics, such as antimicrobial activity and adjustable optical and electronic responses, making them suitable for use in electronics, energy storage, and biomedical devices [5]. LIBS provides an effective means to investigate the influence of laser parameters on plasma behavior during ablation, ultimately contributing to better interpretation of emission characteristics and material response [6].

Previous research has explored how different laser parameters affect plasma formation in various substances. For instance, Fornarini et al. [7] analyzed the influence of Nd:YAG laser wavelengths on bronze plasma, while Naeem et al. [8] reported plasma parameters of copper using a 532 nm laser. However, there is limited literature focusing on the LIBS-based analysis of Zn:Cu alloys under varying laser energies.

This study aims to fill that gap by examining the LIBS spectra of Zn:Cu alloys with a composition ratio of x = 0.9, subjected to laser energies ranging from 400 mJ to 800 mJ. Rather than evaluating energy alone, we emphasize the significance of energy fluence (J/cm²), which considers the actual irradiated surface area and offers a more accurate reflection of plasma formation conditions. The investigation focuses on the role of laser energy and fluence in modulating plasma properties, including electron temperature, electron density, and emission line intensities, to better understand the ablation process and plasma dynamics in Zn:Cu alloys.

2. Experimental Setup

The experimental configuration for LIBS analysis is illustrated in Figure 1. A Q-switched Nd:YAG laser (1064 nm fundamental wavelength, 10 ns pulse duration, 6 Hz repetition rate) was employed to generate plasma on the sample surface. The laser pulse energy was varied between 400 and 800 mJ, and the beam was directed perpendicularly onto the surface of the pelletized target using a system of mirrors and focusing lens. The laser was focused using a plano-convex lens (focal length = 100 mm) to a spot size of ~1 mm diameter on the sample surface, corresponding to energy fluence values in the range of ~50–100 J/cm² depending on the pulse energy.

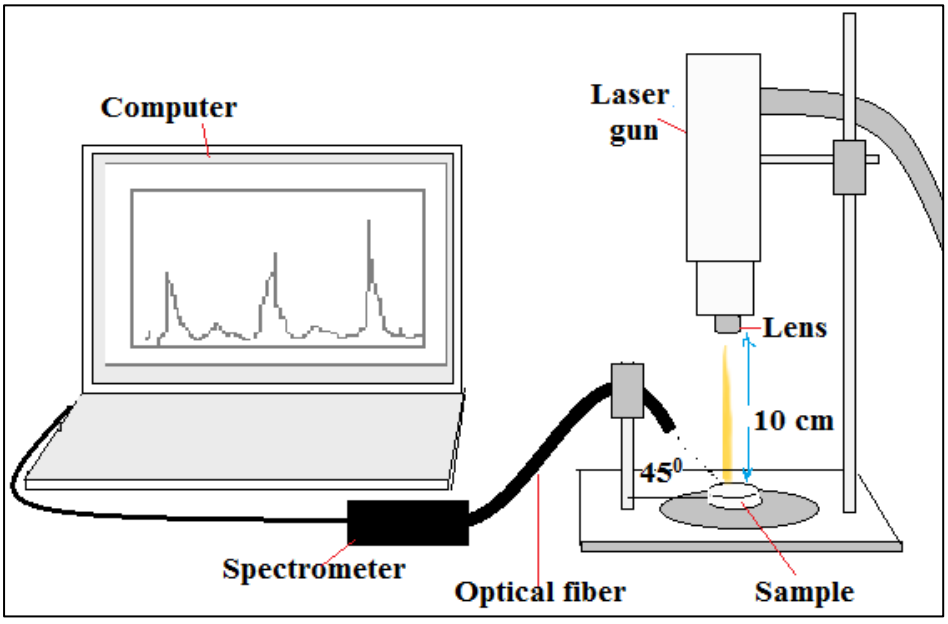

Figure 1: A schematic diagram of the LIBS system.

The target material consisted of a mixture of zinc (Zn) and copper (Cu) powders, with mass ratios of Zn: 0.2 and Cu: 1.79. High-purity Zn (99.9%) and Cu (99.9%) powders were physically mixed without pre-sintering. The powders were thoroughly mixed and compressed into pellets using a hydraulic press operating at 6 Pa for 10 minutes. The resulting pellets had a diameter of 20 mm and a thickness of approximately 10 mm, depending on the compacted material mass (typically 2 g per pellet).

The plasma emission was collected at a 45° angle relative to the laser beam axis using an SMA905 optical fiber, positioned approximately 10 cm from the plasma plume. The collected light was transmitted to a Surwit S3000-UV-NIR spectrometer, which is equipped with a UV-enhanced CCD detector (TCD1304), a 30 μm entrance slit, and a dual blazed grating (600 lines/mm at 250 nm and 750 nm). The spectrometer covers a wavelength range of 190–1100 nm with a typical spectral resolution of ~1 nm (depending on the slit and grating configuration), and a signal-to-noise ratio of 500:1. It includes 16-bit high-precision A/D conversion and 99.8% CCD linearity correction. According to the manufacturer specifications, the minimum exposure time is 0.01 ms, and the maximum exposure time is 60 s.

3. Result and discussion

Figure 2 displays the emission spectra obtained from the Zn:Cu target using laser energies ranging from 400 to 800 mJ. The emission lines were identified using the NIST Atomic Spectra Database, confirming the presence of both neutral and singly ionized species, specifically Zn I, Zn II, Cu I, and Cu II. This validates that laser-induced plasma was successfully formed, as evidenced by the excitation and ionization of the constituent elements. Although the Nd:YAG laser has a photon energy of approximately 1.17 eV (corresponding to a wavelength of 1064 nm), the plasma formation can be attributed to nonlinear absorption mechanisms such as multiphoton ionization and avalanche ionization. These processes allow the laser energy to exceed the ionization potentials of Cu (7.726 eV) and Zn (9.394 eV), thereby generating a plasma plume. The spectra were acquired in free-running mode without the use of gating or temporal delay. As a result, the recorded emission includes both the early-stage continuum background and recombination effects. This approach was intentionally adopted to monitor the full evolution of the plasma emission, particularly the transition from broadband continuum to discrete spectral lines. The influence of this acquisition strategy is discussed in more detail in relation to the observed line intensities and background structure throughout the energy range used.

The spectra in Figure 2 exhibit prominent emission lines in the visible region, particularly between 475–485 nm. While LIBS commonly reveals lines in the ultraviolet (UV) region, the present study focuses on the visible range due to spectrometer limitations. The increasing intensity of spectral lines with laser energy reflects enhanced excitation and ablation at higher pulse energies. Peak labeling has been added, and emission lines were identified based on their known wavelengths and transition probabilities. No self-absorption effects were observed, and the instrumental broadening was subtracted during the Lorentzian fitting procedure.

Moreover, spectral line behavior at higher energies revealed that ionized species (Zn II, Cu II) become more prominent. This behavior reflects enhanced electron impact ionization due to increased electron temperatures and confirms a higher degree of plasma excitation.In Figure 3, the electron number density (n_e) was calculated using the Stark broadening of the Zn I 481.05 nm line according to the relation:

$$n_e = (\Delta\lambda_{1/2} / \omega) \times N_r \quad (1)$$

where $\Delta\lambda_{1/2}$ is the FWHM, ω is the electron impact parameter from NIST, and N_r is the reference density.

As shown in Table 1, the electron density increased from 1.000×10^{18} to 1.121×10^{18} cm^{-3} with rising laser energy, consistent with stronger plasma excitation. These values satisfy the Mc Whirter criterion for LTE, confirming the local thermodynamic equilibrium assumption for subsequent analysis. The moderate increase in n_e despite increasing laser energy may be attributed to plasma expansion and enhanced recombination rates at higher fluence levels, which counteract the generation of free electrons.

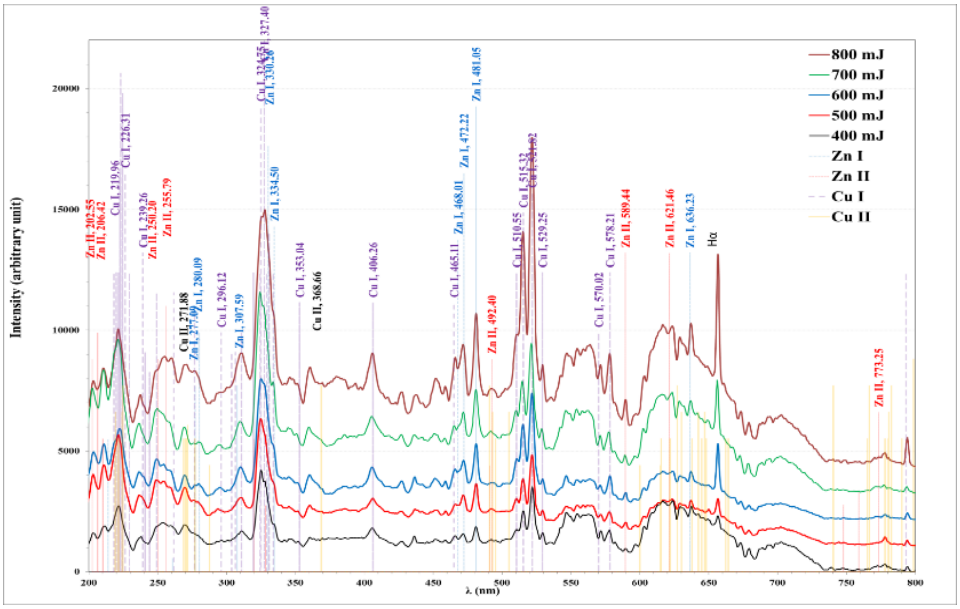

Figure 2: The spectra from laser-induced discharge from the Zn:Cu target using different pulse energies.

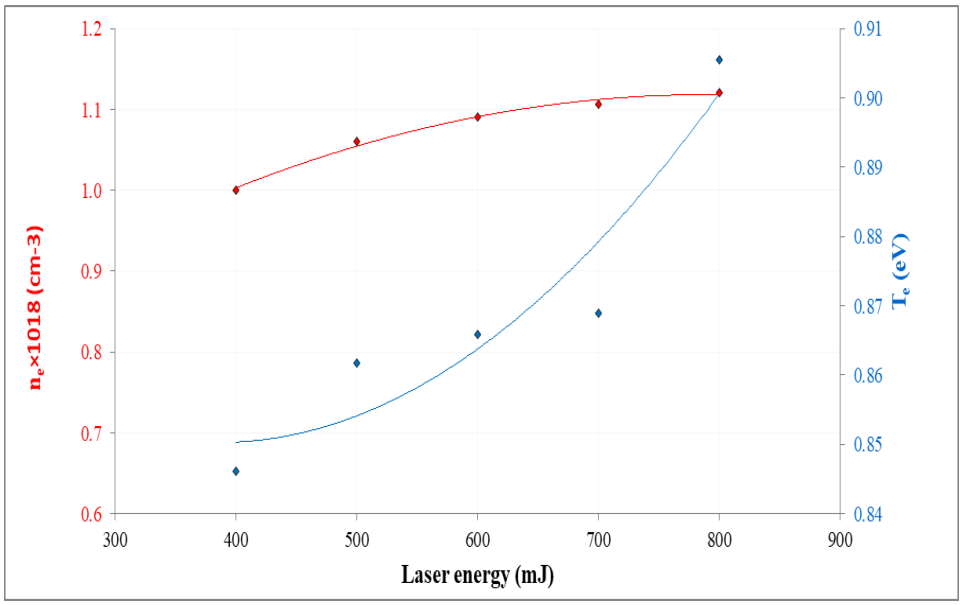

Figure 3: MIPJ electron temperature T_e and density n_e as a function of laser energy.

In Figure 4, the Boltzmann plot method was applied to determine the electron temperature (T_e) from selected emission lines of copper. A linear regression was performed using the equation: ln (λji Iji / hc Aji gj). The negative slope of each fitted line represents the inverse of the electron temperature. The electron temperature (T_e) was calculated using the Boltzmann equation:

$$(Iij\ \lambda ij\ /\ Aij\ gj) = -Ej\ /\ kT_e + \text{constant} \qquad (2)$$

where I_{ij} is the measured intensity of the emission line, $\lambda_{(ij)}$ is the wavelength, $A_{(ij)}$ is the transition probability, g_j is the statistical weight of the upper level, E_j is the excitation energy of the upper level, and k is Boltzmann's constant. The slope of the linear fit equals $-1/kT_e$, allowing direct estimation of the electron

temperature. From the plot, T_e was estimated to be within the range of 0.846 to 0.906 eV, which is consistent with the results obtained from the Stark analysis in Figure 3. This consistency confirms the reliability of both methods and supports the assumption of LTE. The high values of coefficient of determination ($R^2 > 0.98$) indicate a strong linear relationship and validate the applicability of the Boltzmann approach. Uncertainties from line fitting and instrumental effects were considered negligible compared to physical broadening. The observed slow increase in T_e, even with doubling the pulse energy, suggests that significant of the input energy are dissipated via radiative losses, shielding effects, and plasma plume expansion, limiting further electron heating. These energy saturation effects are common in dense laser-induced plasmas and are supported by prior studies [12].

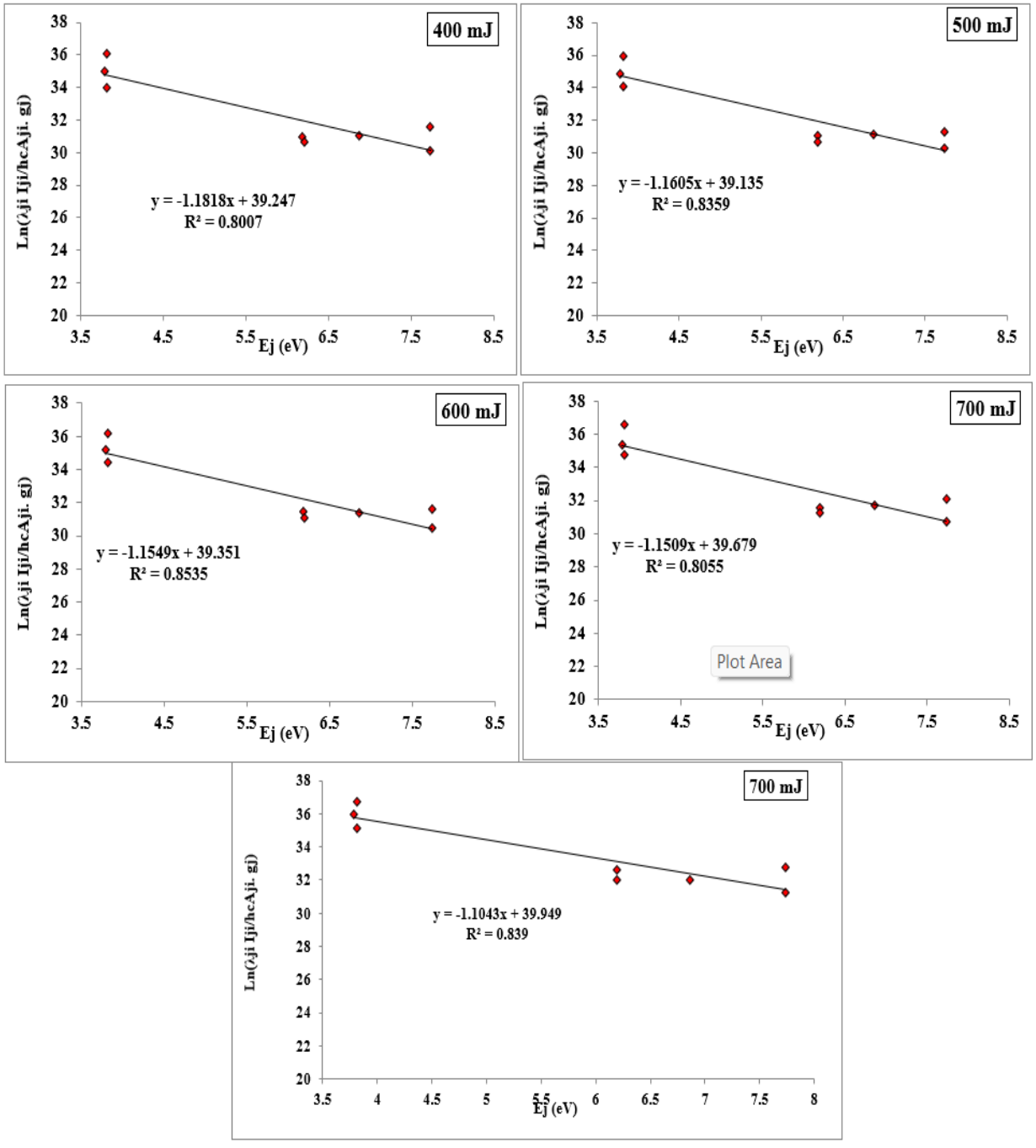

Figure 4: Boltzmann plot utilizing the atomic emission lines of copper.

Figure 5 presents Lorentzian fits for the Zn I line at 481.05 nm across different laser energies. The line shape remains symmetric, justifying the use of Lorentzian profiles. The FWHM values increase with higher laser energy, which directly correlates with increasing electron density. No Doppler or
Van der Waals broadening was significant under these conditions, as estimated from plasma temperature and species mass.
Plasma frequency (f_p), Debye length (λ_D), and Debye number (N_D) were calculated using the following relations:

$$f_p = \sqrt{(n_e e^2 / \pi m_e)} \quad (3)$$

$$\lambda_D = \sqrt{(\varepsilon_0 k T_e / n_e e^2)} \quad (4)$$

$$N_D = (4/3) \pi n_e \lambda_D^3 \quad (5)$$

Where e is the elementary charge, m_e is the electron mass, ε_0 is the vacuum permittivity, and k is Boltzmann's constant.

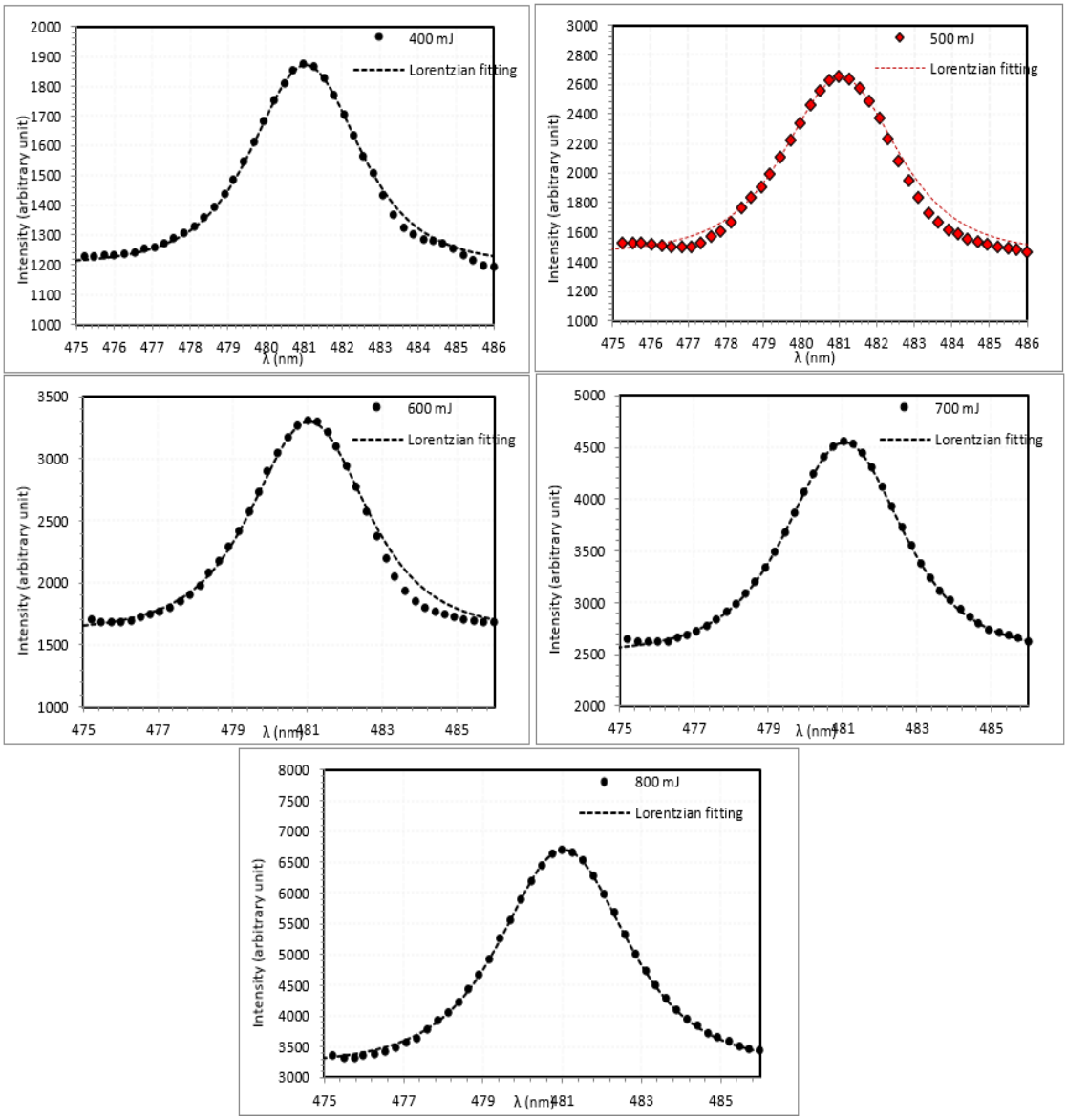

Figure 5: Lorentzian fit of Zn I, 481.05 emitted from the interaction of pulse laser with the Zn:Cu target using different laser energies.

Table 1 also presents calculated plasma parameters including Debye length, plasma frequency, and Debye number. Debye lengths were found to be within the range of $0.683*10^{-5}$cm to $0.668*10^{-5}$ cm, while Debye numbers varied between 1337 and 1398 indicate the plasma was sufficiently large and collisionally dominated, further justifying the LTE assumption.The high values of ND ≫ 1 and plasma frequency values above the electron-neutral collision frequency confirm that the plasma behaves collectively and remains in local thermodynamic equilibrium. These parameters are rarely reported in the context of Zn:Cu systems, thus contributing novel data to LIBS diagnostics.

Overall, the increase in electron temperature from 0.846 ev to 0.906 ev is moderate despite doubling the laser energy, which is explained by energy losses due to expansion and radiation, as reported in similar LIBS studies [12]. This trend aligns with other published work on Zn-based alloys, confirming that most of the excess energy is used for plasma expansion rather than electron heating. Additionally, the consistency of the measured Te and ne with previously reported values for pure Zn, Cu, and other alloys supports the reliability of our measurements and suggests the behavior is characteristic of this material class under nanosecond laser irradiation.

The findings in this study are not only relevant for fundamental plasma physics but also carry implications for LIBS optimization. For instance, understanding the dependence of Te and ne on laser energy allows for tuning ablation conditions to maximize signal intensity and reduce shot-to-shot variation in industrial alloy diagnostics.

Limitations and uncertainties include lack of error bars in the figures and absence of a full spectrometer calibration, which may introduce minor inaccuracies in line position and intensity. Future work should include instrumental error estimation, line overlap correction, and advanced modeling (e.g., Saha-Boltzmann equilibrium).

Table 1: Plasma parameters of LIBS from Zn:Cu targets at different laser energies.

E (mJ)	T_e (eV)	$n_e \times 10^{18}$ (cm^{-3})	f_p (Hz) $\times 10^{10}$	$\lambda_D \times 10^{-5}$(cm)	N_d
400	0.846	1.000	898.000	0.683	1337
500	0.862	1.061	924.812	0.670	1335
600	0.866	1.091	937.930	0.662	1325
700	0.869	1.106	944.421	0.659	1323
800	0.906	1.121	950.868	0.668	1398

The spectral lines used for the Boltzmann and Stark analyses are summarized in Table 2, including their wavelengths, upper-level energies, transition probabilities (A_{ij}), statistical weights (g_i), and Stark broadening constants (ω_s), all obtained from the NIST Atomic Spectra Database.

Table 2: Spectral lines used in Boltzmann and Stark broadening analysis

No.	Element	Wavelength (nm)	Upper Energy Level E_i (eV)	Einstein Coefficient A_{ij} (s^{-1})	g_i	Stark Width ω_s (nm)
1	Zn I	481.05	5.797	1.0×10^8	3	0.032
2	Cu I	510.55	6.19	3.6×10^7	2	0.025
3	Cu I	515.32	6.19	4.5×10^7	4	0.027
4	Cu I	521.82	6.19	3.9×10^7	6	0.03

4. Conclusions

This study demonstrated that increasing the laser pulse energy from 400 mJ to 800 mJ during the ablation of a Zn:Cu (x = 0.9) target led to noticeable changes in plasma characteristics. The electron temperature (Te) increased from 0.846 eV to 0.906 eV, while the electron number density (ne) rose from $1.000*10^{18}$ cm^{-3} to $1.121*10^{18}$ cm^{-3}. These parameters were diagnosed using the Boltzmann plot method for temperature estimation and Stark broadening of emission lines for electron density, ensuring a solid diagnostic foundation.

From a spectral perspective, there was a clear enhancement in the intensity of neutral Zn I lines, along with the emergence of ionized Zn II lines at higher energies, indicating stronger excitation and ionization processes as laser energy increased.

In addition, the Debye length (λD) decreased from $0.683*10^{-5}$ cm to $0.668*10^{-5}$cm, while the Debye number (Nd) increased, implying a transition toward a more compact and quasi-equilibrated plasma state. These changes also support the assumption of local thermodynamic equilibrium (LTE) under the studied conditions.

It is important to note that this work relied on time-integrated spectra, which limits the ability to track the temporal evolution of plasma parameters. Furthermore, the analysis was conducted under the LTE assumption, which may not fully hold across all spatial and temporal domains of the plasma plume.

These findings emphasize the critical role of laser energy in tuning plasma properties and provide a quantitative framework for optimizing Laser-Induced Breakdown Spectroscopy (LIBS) performance. The observed trends can be instrumental in enhancing the analytical sensitivity, repeatability, and reliability of LIBS, especially for alloy characterization and material diagnostics.

In conclusion, this study confirms that plasma characteristics can be deliberately controlled by adjusting laser pulse energy, reinforcing the value of LIBS as a powerful tool for elemental analysis and real-time process monitoring in both scientific and industrial applications.

References

[1] P. Li, Z. Xiong, Z. Ma, J. Guo, and C. Wang, "Analysis of Cu and Zn contents in aluminum alloys by femtosecond laser-ablation spark-induced breakdown spectroscopy", Open Physics, 21, 113–123 (2023).
[2] S. F. Khaleel and K. A. Aadim, "Investigation study of the plasma parameters for bronze produced by Nd:YAG laser at wavelength 1064 nm: effect of laser energies", Journal of Optics, 54, 256–266 (2025).
[3] Z. M. Abbas and Q. A. Abbas, “Characterization of magnetized-plasma system induced by laser,” Iraqi Journal of Physics, vol. 21, no. 4, pp. 45–55, 2023, doi: 10.30723/ijp. v21i4.1148.
[4] R. S. Mohammed, K. A. Aadimi, and K. A. Ahmed, "Spectroscopy diagnostic of laser intensity effect on Zn plasma parameters generated by Nd: YAG laser," Iraqi Journal of Science, vol. 63, no. 9, pp. 3711–3718, 2022, doi: 10.24996/jjs.2022.63.9.5.
[5] F. H. Salih, S. S. Mahdi, A. H. Ali, “Employment of laser induced breakdown spectroscopy to determine elements of human hair,” Baghdad Science Journal, vol. 22, no. 3, pp. 946–954, 2025 (published online first 20 Oct 2024), doi: 10.21123/bsj.2024.10388.
[6] D. A. Cremers and L. J. Radziemski, Handbook of Laser-induced breakdown spectroscopy, 2nd ed., Wiley (2021).
[7] D. W. Hahn and N. Omenetto, "Laser-induced breakdown spectroscopy (LIBS), part II: Review of instrumental and methodological approaches", Applied Spectroscopy, 66, 347–419 (2012).
[8] F. F. Chen, Introduction to plasma physics and controlled fusion, 2nd ed., Springer, 2012.
[9] E. Mal, R. Junjuri, M. K. Gundawar, and A. Khare, "Optimization of temporal window for application of calibration free-laser induced breakdown spectroscopy (CF-LIBS) on copper alloys in air employing a single line", Journal of Analytical Atomic Spectrometry, 34, 319–330 (2019).
[10] M. S. Mahde, A. H. Ali, M. H. Hussein, “Diagnostic study of copper plasma in air by laser induced breakdown spectroscopy (LIBS),” Engineering & Technology Journal, vol. 33, Part A, no. 5, pp. 1002-1008, 2015, doi: 10.30684/etj.33.5A.18.
[11] J. Iqbal, T. A. Alrabdi, A. Fayyaz, H. Asghar, S. K. H. Shah, and M. Naeem, "Elemental study of Devarda’s alloy using calibration free-laser induced breakdown spectroscopy (CF-LIBS)", Laser Physics, 33, 025701 (2023).
[12] C. Aragón and J. A. Aguilera, "Characterization of laser induced plasmas by optical emission spectroscopy: a review of experiments and methods", Spectrochimica Acta Part B: Atomic Spectroscopy, 63, 893–916 (2008).

[13] G. Cristoforetti, S. Legnaioli, L. Palleschi, and V. Palleschi, "Local thermodynamic equilibrium in laser-induced breakdown spectroscopy: beyond the McWhirter criterion", Spectrochimica Acta Part B: Atomic Spectroscopy, 65, 86–95 (2010).
[14] Z. Hou, Y. Zhang, and X. Li, "A calibration-free model for laser-induced breakdown spectroscopy using non-gated detectors", Frontiers of Physics, 17, 115 (2022).
[15] A. Kramida, Y. Ralchenko, J. Reader, and NIST ASD Team, "NIST Atomic Spectra Database (ver. 5.3)", National Institute of Standards and Technology, Gaithersburg, MD (2015).

تقييم كمي لتأثير طاقة نبضة الليزر على خصائص بلازما Zn–Cu باستخدام تشخيصي بولتزمان وستارك

سنا عبد اللطيف صالح[1]،* و كاظم عبدالواحد عادم[2]

[1] قسم الفيزياء، كلية العلوم، جامعة بغداد، بغداد، العراق
[2] معهد الليزر للدراسات العليا ،جامعة بغداد، بغداد، العراق

البريد الالكتروني للباحث: Sanaa.Abd2304@sc.uobaghdad.edu.iq

الخلاصة: في هذه الدراسة، تم استخدام التحليل الطيفي لانهيار البلازما الناتج بالليزر (LIBS) لتحليل البلازما المتولدة من سبيكة الزنك والنحاس (Zn:Cu) بنسبة (x = 0.9)، باستخدام ليزر Nd:YAG بطول موجي 1064 نانومتر. تم توليد البلازما عند طاقات نبض ليزر مختلفة تتراوح من 400 إلى 800 ميلي جول. تم تحديد درجة حرارة الإلكترونات (Te) باستخدام طريقة مخطط بولتزمان، بينما تم حساب كثافة الإلكترونات (ne) باستخدام ظاهرة اتساع ستارك. كما تم تقييم معلمات بلازما أخرى، بما في ذلك تردد البلازما (fp)، وطول ديباي (λD)، وعدد ديباي (Nd).
أظهرت النتائج أن درجة حرارة الإلكترونات ارتفعت من 0.846 إلكترون فولت عند 400 ميلي جول إلى 0.906 إلكترون فولت عند 800 ميلي جول، كما ارتفعت كثافة الإلكترونات من 1.000×10^{18} سم$^{-3}$ إلى 1.121×10^{18} سم$^{-3}$. وازداد تردد البلازما من 898.000×10^{10} هرتز إلى 950.868×10^{10} هرتز، في حين انخفض طول ديباي قليلاً من 0.683×10^{-5} سم إلى 0.668×10^{-5} سم. وأظهر عدد ديباي تغيراً طفيفاً حول القيمة 1300، مما يعكس سلوكاً جماعياً مستقراً نسبياً عبر نطاق الطاقة المستخدم.
تشير هذه النتائج إلى أن زيادة طاقة الليزر تؤدي إلى توليد بلازما أكثر حرارة وكثافة، مما يعزز شدة الانبعاث وخصائص البلازما. وتُسهم هذه الدراسة في تقديم رؤى كمية حول سلوك بلازما Zn–Cu تحت تأثير طاقات ليزر مختلفة، مما يوفر تطبيقات محتملة في تشخيص المواد باستخدام تقنية LIBS.